



Cadmium Doped Copper Containing Phosphate Glass as a Bandpass Filter for Solar Cell Protection

H. A. Abd El-Ghany

Department of Engineering Mathematics and Physics, Faculty of Engineering (Shoubra), Benha University, Cairo, 11629, Egypt.

hytham.abdelghany@feng.bu.edu.eg

ABSTRACT

A glass system of composition $44\text{P}_2\text{O}_5-38\text{ZnO}-2\text{CuO}-(16-x)\text{Na}_2\text{O}-x\text{CdO}$ (where, $x = 1, 2, 3, 4,$ and 5 mol%) has been prepared using the conventional melt quenching technique. XRD patterns confirmed the amorphous nature for the prepared samples. Archimedes' method was used to determine the density of the prepared glass samples then the molar volume was calculated. The optical spectroscopic investigations of the prepared glass samples were carried out over the spectral range (190-1100 nm). The transmission spectra revealed that the prepared glass samples behave as bandpass filters in the visible region. The absorption studies were employed to determine the optical band gap and Urbach energy. The spectral distribution of the refractive index assured the lowest dispersion of the glass in the visible region. Other physical parameters such as the extinction coefficient, the optical conductivity, and the complex dielectric constant were evaluated. The results suggested the practicality of employing such low-cost glass as a bandpass filter for optical applications such as UV-elimination and solar cell protection. The role of CdO as a network modifier in the phosphate glass was revealed.

KEYWORDS:

Phosphate glass, CdO, bandpass filter, optical band gap, Urbach energy.

Language: English

Date of Publication: 30-06-2018

DOI: 10.24297/jap.v14i2.7450

ISSN: 2347-3487

Volume: 14 Issue: 2

Journal: Journal of Advances in Physics

Website: <https://cirworld.com>



This work is licensed under a Creative Commons Attribution 4.0 International License.



1. INTRODUCTION

The competition of practicality, low cost and reliability of glasses in different applications has opened the field of research for new compositions which meet the specific requirements [1-3]. Compared with other glass formers such as silicate and borate systems, phosphate glasses offer simple composition, low melting and softening temperatures with strong glass forming character. Besides this they have high electrical conductivity, high thermal expansion coefficients, low thermal conductivity and low dispersion [4-6]. Nevertheless, poor chemical durability of phosphate glasses is a great disadvantage for utilizing this type of glass; which limits its use in many applications [7]. Many of the physical properties of phosphate glasses can be greatly changed by the addition of a precisely amount of modifiers [8-10]. However, Sodium phosphate glasses have evidence of low melting point, high ionic conductivity, and strong glass-forming character [11]. Moreover, ZnO can be added as a good modifier to enhance the chemical durability of phosphate glasses since zinc ion acts as a strong ionic cross linker between host phosphate anions i.e. inhibits the hydration reaction [12,13].

Particular attention has been paid to the copper doped phosphate glasses because of their semiconducting properties, interesting optical transmission/absorption spectrum and relatively low glass transformation temperature [14]. CuO can greatly modify the absorption behavior of phosphate glass because it has two optical absorption bands at the ultraviolet and visible-near infrared regions of spectrum, i.e. producing bandpass filters [15-18]. From point of interest, cadmium comes as a divalent metal which act as a network former or modifier depending upon the chemical composition and the host material. It stabilizes the glass structure as well as modifies the optical and electronic properties of the host glasses [19]. Consequently, cadmium can be used as a coloring, phase separation, and photoconductive material [20,21]. Because of its high density and low binding energy, cadmium is used in quantum dot solar cells [22]. However, the coupling between cadmium and copper in phosphate-based glasses can be of potential interest as bandpass filters. The center and width of the bandpass filter in addition to its color play the most important role in controlling the light pass [23].

Apart from these, photovoltaic (PV) modules are of great significance as an important technique by which the solar energy is converted to electricity by means of solar cells. Intensive efforts are being made to enhance the conversion efficiency of the solar cells as well as reduce the cost of their production. However, the performance of the PV modules is greatly affected by many parameters including exposure to ultraviolet (UV) and infrared (IR) radiations. Many observations have demonstrated a degradation effect due to ultraviolet portion of solar radiation which is termed UV-induced degradation. This degradation begins directly after first exposure to the light, leading to reduce the conversion efficiency of the PV module and shorten the life time of the solar cell [24-26]. Such degradation can be prevented by using glass substrates which block the UV radiation below 350 nm [27]. On the other hand, IR radiation being a wide portion of the solar spectrum disturbs the working of the PV module due to its thermal effect. In most conventional solar cells this part of solar radiation is not converted into electricity and appears as thermal energy which leads to an increase in the ambient temperature of the solar cell. Many studies indicate that the conversion efficiency of the solar cells is decreased by increasing their working temperature [28,29].

The present study suggests a solution to the above-mentioned problem by proposing a low- cost glass system which can work as a bandpass filter in visible region of spectrum in order to protect the solar cells. In other words, the glass permits the transmission of visible light and at the same time absorbs the UV and IR radiations to prevent the degradation and heating effects within the solar cell respectively. The present work proposed a glass system with the chemical composition $44\text{P}_2\text{O}_5\text{-}38\text{ZnO-}2\text{CuO-}(16\text{-}x)\text{Na}_2\text{O-}x\text{CdO}$ (where, $x = 1, 2, 3, 4,$ and 5 mol%). According to available knowledge, no data has been reported for cadmium-copper-phosphate glasses in optical filters applications. Consequently, the role of cadmium on the physical and optical properties of the suggested glass system is discussed.



2. EXPERIMENTAL METHOD

A glass system with chemical composition $44\text{P}_2\text{O}_5\text{-}38\text{ZnO}\text{-}2\text{CuO}\text{-}(16\text{-}x)\text{Na}_2\text{O}\text{-}x\text{CdO}$ (where, $x = 1, 2, 3, 4,$ and 5 mol%) has been prepared by the conventional melt quenching technique. Analytically pure grade of the chemicals $\text{NH}_4\text{H}_2\text{PO}_4$, ZnO , CuO , NaCO_3 , and CdO were used. After weighing the required amount of materials, they were mixed and grinded using mortar for 30 minutes. The mixture in a porcelain crucible was put in a muffle furnace for 1 hour at 250°C to release the gases such as CO_2 and NH_3 . The crucible was then placed in a melting furnace for 1 hour at 1000°C , and shaken clockwise to ensure the maximum homogeneity of the mixture. Finally, the casting was quenched and annealed at 250°C using stainless steel mould with pressing plate to obtain thin disks in order to perform the optical measurements. The annealing process is an important step required to remove the internal stress that remains within the prepared glass during the quenching process. The amorphous nature of the obtained transparent samples was identified by means of X-ray diffraction (XRD) technique. The diffraction data were recorded for 2θ values between 4° and 70° .

The glass samples were produced almost as disks of diameters ≈ 2.75 cm. The glass density was measured at room temperature using the conventional Archimedes' method, with toluene as an immersion liquid of stable density (0.868 g/cm^3) as [15-17]:

$$\rho = \frac{W_{air}}{(W_{air}-W_{liq})} \rho_o \quad (1)$$

Where, W_{air} and W_{liq} are the weights of the sample in air and in liquid respectively. The molar volume was calculated from the molecular weight, M_w and the density, ρ as [30]:

$$V_M = \frac{M_w}{\rho} \quad (2)$$

The optical absorption and transmission spectra were measured at room temperature using UV/VIS absorption (JASCO V570) spectrophotometer over the wavelength range (190-1100 nm).

3. RESULTS AND DISCUSSIONS

3.1. XRD Investigation

Figure 1 shows the X-ray diffraction patterns of the prepared samples with different mol% of CdO content. The results of XRD studies of all samples show diffused scattering where broad humps can be observed. The absence of Bragg's peaks in the XRD pattern confirms the amorphous nature of the prepared samples. Moreover, the broad profiles around $2\theta = 30^\circ$ suggest the existence of some short-range order in the glass samples [31].

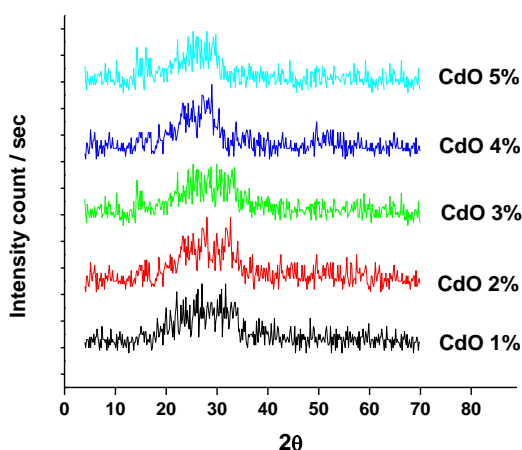


Fig. 1: XRD patterns of glass samples for different CdO content.



3.2. Density and Molar volume Measurements

The density and molar volume measurements are considered to be very important tools to detect the structural changes and the arrangement of the building units in the glass network. Equations (1) and (2) have been employed to calculate the density, ρ and molar volume, V_M of the glass samples respectively. The resulting values of the density and the corresponding molar volume as a function of CdO concentration are listed in Table 1. The results indicate a linear increase in the density of the glass samples with increasing content of CdO. However, the molar volume is found to have the opposite trend to that of the density as shown in Fig. 2. The increase in density agrees qualitatively with that predicted by the composition relation in which the low density Na_2O (2.27 gm cm^{-3}) was replaced by the high density CdO (8.15 gm cm^{-3}) [32]. The ionic concentration, N and the inter-ionic distance, r_i of the glass system can be determined using the relations [33]:

$$N(\text{ions}/\text{cm}^{-3}) = \frac{(\text{Avogadro's No.}) (\text{mole\% of cation}) (\text{glass density})}{(\text{glass average molecular weight})} \quad (3)$$

$$r_i(\text{A}^\circ) = (1/N)^{\frac{1}{3}} \quad (4)$$

The calculated values of Cd-ion concentration and the corresponding inter-ionic distance of the glass samples are listed in Table 1. It can be observed that Cd-ion concentration increases whereas inter-ionic distance decreases with increasing concentration of CdO which is consistent with the obtained behavior of the density and molar volume. The results suggest the role of CdO as a network modifier of $44\text{P}_2\text{O}_5\text{-}38\text{ZnO-}2\text{CuO-}(16\text{-}x)\text{Na}_2\text{O-}x\text{CdO}$ glass system.

Table 1. Density, molar volume, ionic concentration and inter-ionic distance of prepared glass samples.

CdO content (mole %)	Density, ρ (g/cm^3)	Molar volume, V_M (cm^3/mole)	Ionic concentration, N ($10^{20} \text{ ion}/\text{cm}^3$)	Inter-ionic distance, r_i (A°)
1%	3.0374	33.6411	1.79	17.74
2%	3.0655	33.5488	3.59	14.07
3%	3.0946	33.4487	5.40	12.28
4%	3.1171	33.4200	7.21	11.15
5%	3.1446	33.3392	9.03	10.34

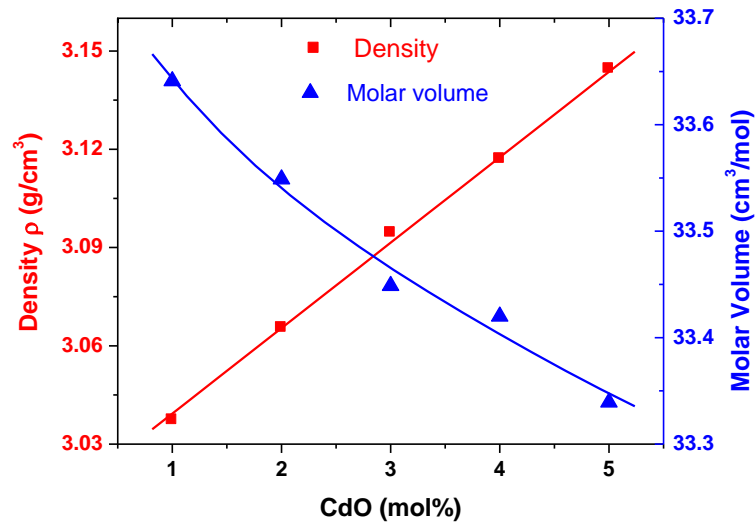


Fig. 2: Variation of density and molar volume with respect to CdO content.

3.3. Optical Studies

3.3.1. Absorption and Transmission Spectra

The optical absorption and transmission studies in the UV-visible range have been carried out over the wavelength range (190-1100 nm). The optical absorption spectroscopy is very helpful in studying the optically induced transitions and presenting an insight in the band structure of crystalline and amorphous materials. In crystalline solids there are a well-defined energy bands having a sharp lattice absorption edge whereas amorphous materials exhibit tailing into the normally forbidden energy gap i.e. the absorption edge has finite slope [34,35]. Figure 3 shows the absorption spectra of glass samples for different CdO concentrations. The absence of sharp absorption edge in the optical spectra reveals the amorphous nature of the glass samples. It can be observed that the absorption increases with increasing CdO concentration where all samples show two highly absorption bands in the ultraviolet and near-infrared regions. This is most likely related to the coupling between the CdO and CuO. The transmission spectra of the glass samples with different concentrations of CdO are shown in Fig. 4. It can be indicated that all spectra follow one common pattern where a single broad transmission band in the visible region can be observed. The transmission spectra are found to be in agreement with the obtained absorption data. The results reveal that the prepared glass samples can serve as bandpass filters with a sufficiently transmission of visible light. A general decrease in transmittance with increasing concentration of CdO is observed, which can be attributed to the change in the glass composition where Na₂O is replaced by the heavier CdO. It can be quite clear that both optical absorption and transmission of the prepared samples are strongly dependent on the glass composition i.e. CdO content.

3.3.2 Bandpass Filter Parameters

It must be mentioned that the transmitted energy through the bandpass filter is worthily controlled by several parameters of the transmission band such as the peak height, position, broadening and area. All these parameters are found to be greatly dependent on the glass composition as indicated in Table 2. The center of the transmission band is found to be shifted from 512 nm to 535 nm with increasing concentration of CdO which may be related to the coupling between CuO and CdO. It can be concluded that the addition of CdO disturbs the ligand field around the Cu²⁺ probe ion. This shift towards the higher wavelengths is very useful in changing the color of the obtained bandpass filters for industry requirements. Figure 5 show the UV band stop of the prepared glass samples from which the UV cutoff wavelength is found to be increased from 323 nm to 360 nm by increasing concentration of CdO. The red shift in the absorption edge or UV cutoff can be



attributed to the progressive increase in the number of non-bridging oxygens (NBOs) [36]. This can be understood on the basis that a monovalent Na^+ ion in the form of Na_2O disrupts one bridging oxygen in the phosphate network, i.e. creates only one non-bridging oxygen. Meanwhile, introducing of a divalent Cd^{2+} ion into the phosphate network in the form of CdO disrupts two bridging oxygens, i.e. creates two non-bridging oxygens. Thus, by increasing of CdO content, creation of greater number of NBOs seems to be the reason for the shift of the absorption edge towards higher wavelengths. The results reveal that the present glass system can be considered as a good candidate in UV-elimination techniques. Moreover, it is evident from the transmission spectra of all samples that the near IR band above 750 nm is attenuated to about 10% transmittance. Well, blocking the UV radiation below 360 nm along with attenuation of almost IR radiation above 750 nm suggest the use of the present glass system as a protective agent in the solar cells to eliminate the undesirable effects of degradation and heating caused by UV and IR radiations respectively. Accordingly, by employing such low-cost glass, the conversion efficiency of the PV module is expected to be larger and the life time of the solar cell is expected to be longer.

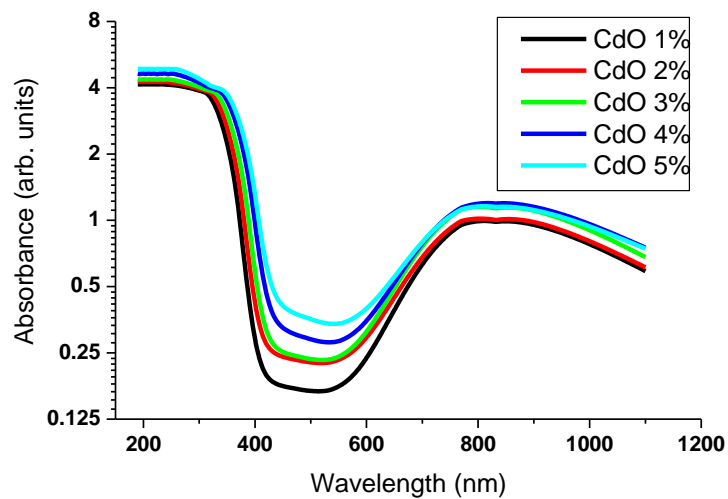


Fig. 3: Absorption spectra of the glass samples for different CdO ratios.

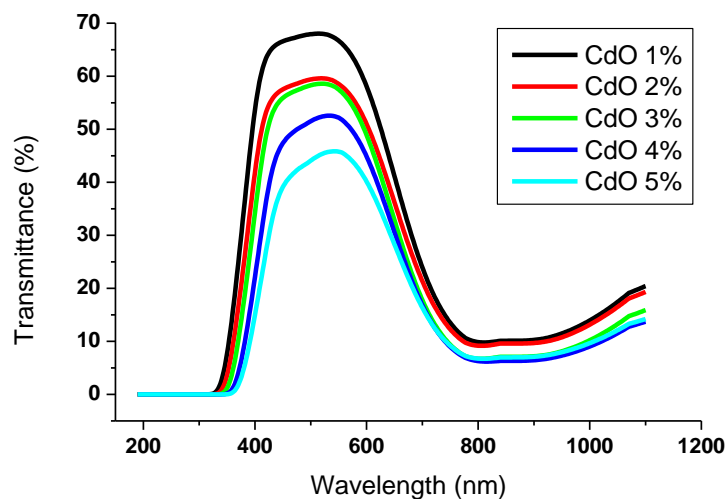


Fig. 4: Transmission spectra of the glass samples for different CdO ratios.



Table 2. The transmission band analysis of the bandpass filter.

CdO content (mole %)	UV band stop (nm)	Center (nm)	Width (nm)	Area (a.u.)	Height (%)
1%	190 – 323 nm	512	260	20379	68.25
2%	190 – 335 nm	516	251	16967	60.12
3%	190 – 344 nm	519	237	15820	58.75
4%	190 – 352 nm	528	229	13440	52.75
5%	190 – 360 nm	535	224	11195	46.11

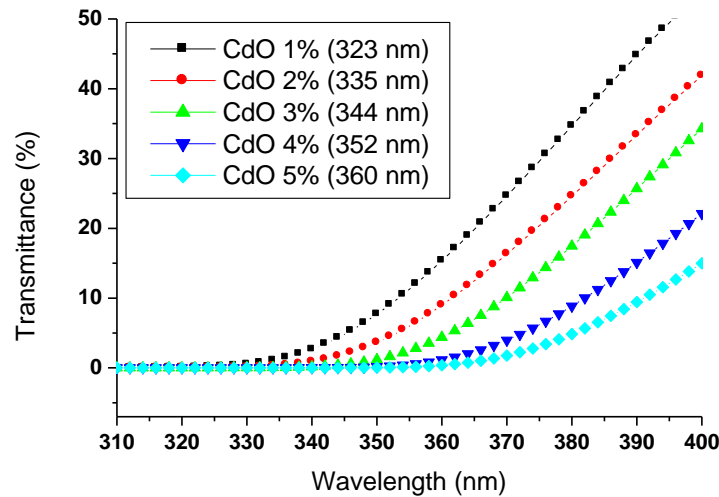


Fig. 5: UV band stop for glass samples for different CdO ratios.

3.3.3. Optical Band Gap and Urbach Energy

The optical band gap is one of the most significant parameters in amorphous semiconducting material. The optical behavior of a material is utilized to provide a picture of the density of states distribution in the energy gap of amorphous solids. The optical band gap, E_g of the glass samples can be determined using the relation [15]:

$$\alpha h\nu = B(h\nu - E_g)^n \quad (5)$$

With, B is constant and α is the absorption coefficient that was calculated by [15,18]:

$$\alpha(\nu) = 2.303 (A/d) \quad (6)$$

Where, A is the absorbance and d is the thickness of the sample. It is convenient in amorphous solids to take $n=2$ which indicates an indirect absorption mechanism [18]. The process is achieved by plotting $(\alpha h\nu)^{1/2}$ as a function of photon energy ($h\nu$) and taking the extrapolation of the straight portion of the graph hence the optical band gap energy is determined as shown in Fig. 6. The calculated values of optical band gap energy are listed in Table 3, where E_g is found to be decreased from 3.26 eV to 2.95 eV by increasing the concentration of CdO. This is most likely due to the progressive increase in number of non-bridging oxygens



(NBOs) by increasing CdO content as mentioned earlier. Therefore, one should expect that the optical band gap energy, E_g and the UV cutoff wavelength have opposite trends as depicted in Fig. 7.

However, the lack of long-range order in non-crystalline materials is associated with the disorder effects caused by the incident photon energies less than the band gap energy. This can be explained by the presence of localized states which form a band tails within the band gap [37]. Calculation of the width of such band tails or the Urbach energy, ΔE yields information about the density of the localized states in the band gap according to the relation [38,39]:

$$\alpha = \alpha_0 \exp(h\nu / \Delta E) \quad (7)$$

With, α is the absorption coefficient and α_0 is constant. As shown in Fig. 8, the Urbach energy can be determined experimentally by plotting $\ln(\alpha)$ as a function of the photon energy ($h\nu$) and taking the reciprocal of the slope of the linear portion of the graph. As listed in Table 3, ΔE is found to be increased from 0.158 eV to 0.172 eV by increasing the concentration of CdO, which indicates an increase of the degree of disorder in the system. It can be conclude that the increase of CdO content localizes some states within the band gap, which seem to be the reason of the observed decrease in the E_g values.

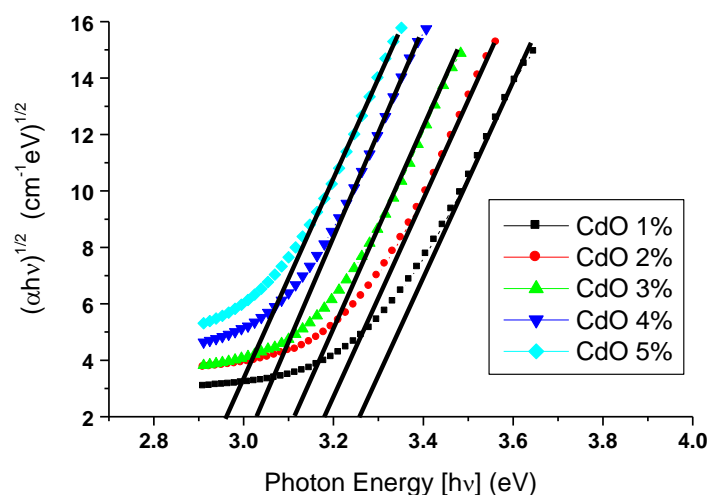


Fig. 6: Determination of the optical band gap energy.

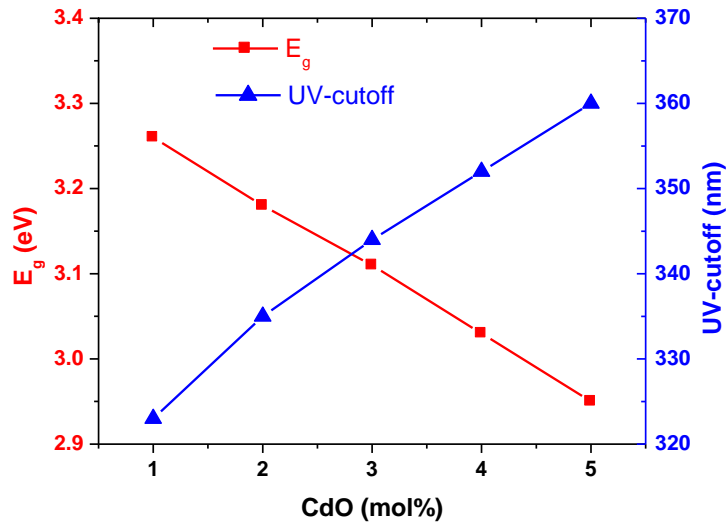


Fig. 7: Optical band gap energy and UV-cutoff wavelength with respect to CdO content.

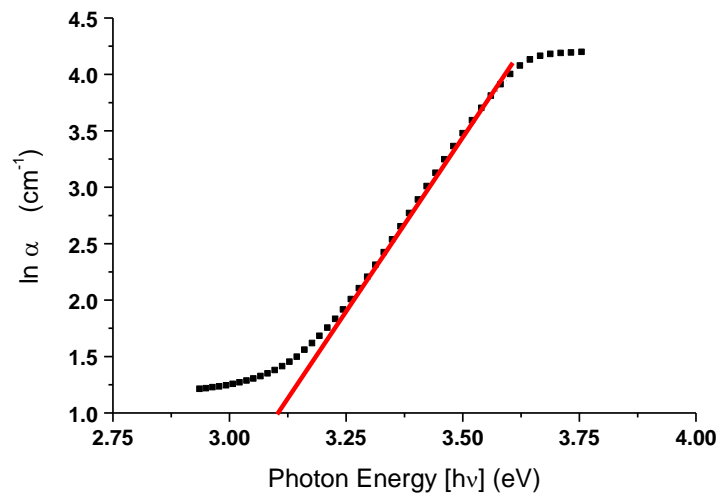


Fig. 8: A representative example for determination of Urbach energy for CdO 1% content.

Table 3. The optical band gap and Urbach energy of the glass samples.

CdO concentration (mole %)	1%	2%	3%	4%	5%
Optical band gap E_g (eV)	3.26	3.18	3.11	3.03	2.95
Urbach energy ΔE (eV)	0.158	0.161	0.162	0.167	0.172



3.4. Essential Physical Parameters

The refractive index is a fundamental property of any optical material. The spectral distribution of the refractive index, n of the glass samples can be determined according to the relation [40]:

$$R = \frac{(n-1)^2}{(n+1)^2} \quad (8)$$

Where, R is the reflectance of the glass samples. As depicted in Fig. 9, a general increase in the refractive index with increasing CdO content is indicated. The calculated values of the refractive index reveal strong wavelength dependence except almost at the visible region where low dispersion can be observed. High depression on both sides of the graph can be attributed to the electronic and molecular polarization frequencies which induce strong absorption [41]. The weakest wavelength dependence of the refractive index can be noticed between 450 nm and 550 nm as shown in Fig. 10. Accordingly, the prepared glass system exhibits the lowest dispersion in this range of visible region. The results indicate an increase in the refractive index values with increasing content of CdO. This is most likely related to the replacement of Na_2O by CdO and consequently, the change in refractive index is attributed to the difference in refraction of Na^+ ion and the heavier Cd^{2+} ion.

Other physical properties such as extinction coefficient, k and optical conductivity, σ can be determined using the relations [42,43]:

$$k = \frac{\alpha\lambda}{4\pi} \quad (9)$$

$$\sigma = \frac{\alpha n c}{4\pi} \quad (10)$$

Where, α is the absorption coefficient, n is the refractive index and c is the velocity of light. The extinction coefficient measures the fraction of radiation lost per unit thickness of the participating glass due to scattering and absorption effects. On the other hand, the optical conductivity provides information about the optical response of this glass. The calculated values of the extinction coefficient and the optical conductivity of the prepared glass samples are depicted in Figs. 11 and 12 respectively where both of them are found to be increased with the increasing content of CdO.

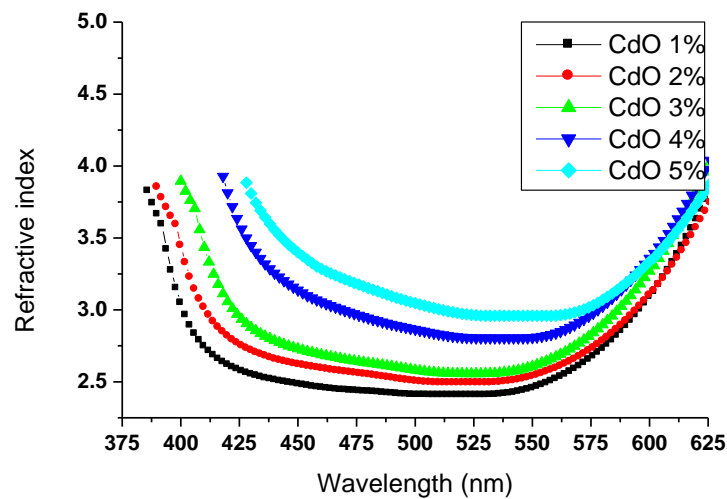


Fig. 9: Wavelength dependence of the refractive index for different CdO content.

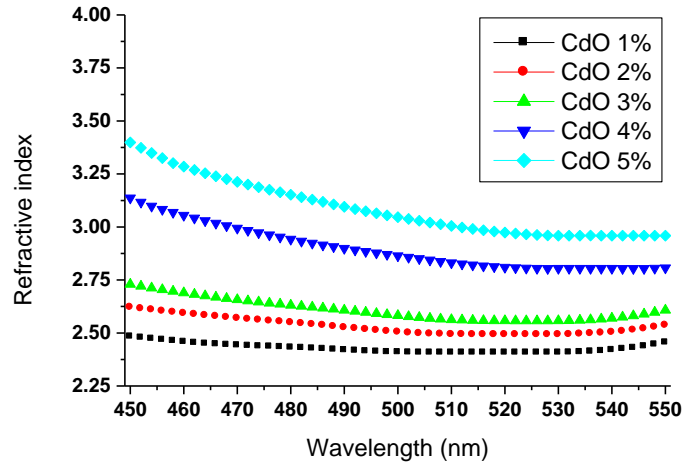


Fig. 10: Refractive index for different CdO ratios.

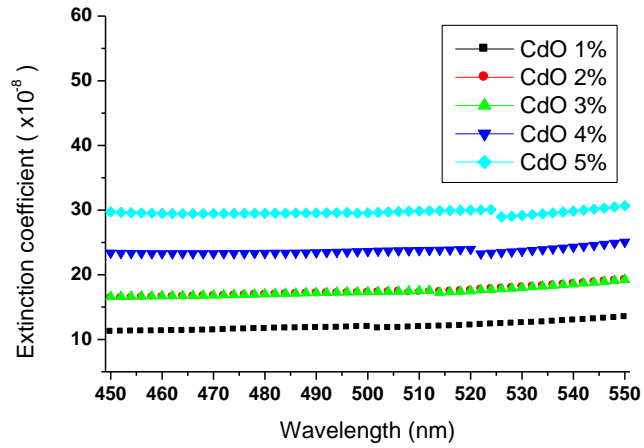


Fig. 11: Extinction coefficient for different CdO ratios.

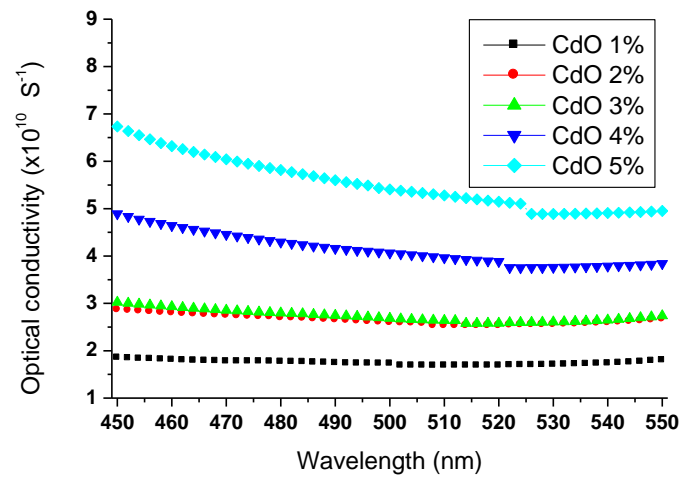


Fig. 12: Optical conductivity for different CdO ratios.



The complex dielectric constant of the prepared glass is a fundamental intrinsic property. The real part of the dielectric constant defines the ability to slow down the light which passing through the material while the imaginary part shows how the material absorbs energy from an electric field due to dipole motion. The ratio of the imaginary part to the real part of the dielectric constant defines the loss factor in a specific material. The real part, ϵ' and imaginary part, ϵ'' of the complex dielectric constant are calculated using the relations [43]:

$$\epsilon' = n^2 - k^2 \quad (11)$$

$$\epsilon'' = 2nk \quad (12)$$

Where, n is the refractive index and k is the extinction coefficient. The calculated values of ϵ' and ϵ'' are depicted in Figs. 13 and 14 respectively where both of the real and the imaginary parts of the dielectric constant exhibit higher values with increasing content of CdO. It is quite clear that the chemical composition of the glass plays the main role in changing of the extinction coefficient, the optical conductivity, the real and the imaginary parts of the dielectric constant. This seems to be associated with certain structural changes occurring in the glass with changing of the composition, i.e replacing of Na_2O by CdO. Again, the results assure the role of CdO as a network modifier in the phosphate glass.

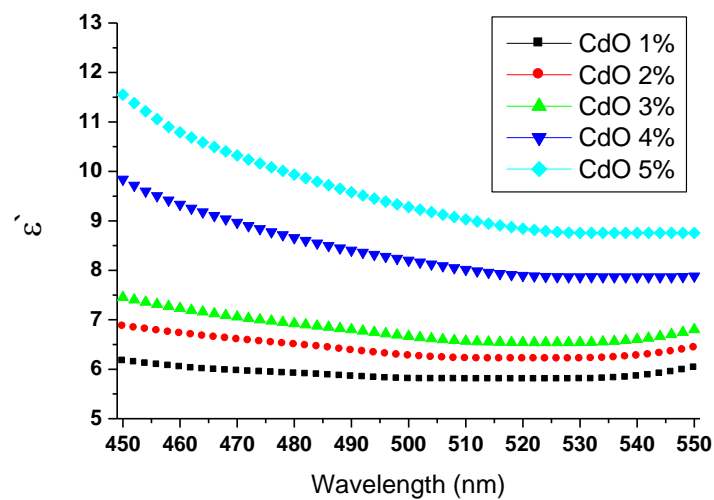


Fig. 13: The real part of the dielectric constant for different CdO ratios.

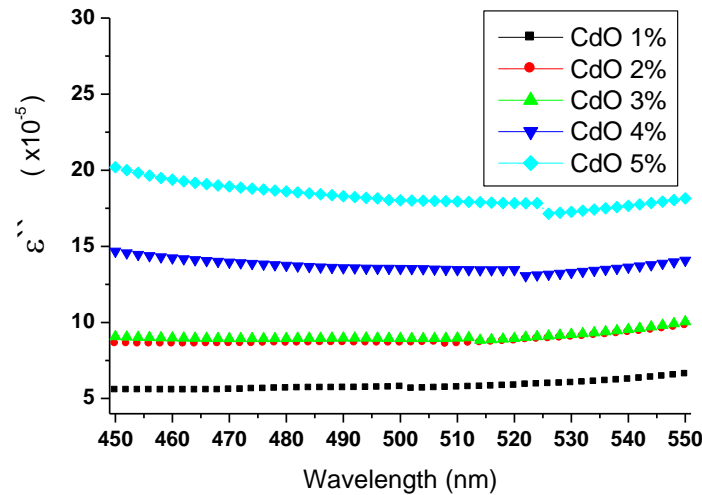


Fig. 14: The imaginary part of the dielectric constant for different CdO ratios.

4. CONCLUSIONS

A glass system with chemical composition $44\text{P}_2\text{O}_5-38\text{ZnO}-2\text{CuO}-(16-x)\text{Na}_2\text{O}-x\text{CdO}$ (where, $x = 1, 2, 3, 4,$ and 5 mol%) has been prepared by the conventional melt quenching technique. The XRD patterns confirm the amorphous nature of the prepared samples. The density of the prepared glass samples is found to be increased by increasing content of CdO while the molar volume exhibits an opposite trend to that of the density. The optical studies revealed that all glass samples behave as bandpass filters in visible region with elimination of UV band below 360 nm and almost IR band above 750 nm. Thus, the prepared glass can be practically used as a UV-preventing element. In addition, it can be used as a protective agent in the solar cells to eliminate the undesirable effects due to degradation and heating of the PV module. In this way, the conversion efficiency and the life time of the solar cell can be greatly enhanced. The optical band gap is found to be decreased from 3.26 eV to 2.95 eV with increasing content of CdO. On the other hand, the width of the band tailing worked out from the Urbach plots is found to be increased from 0.158 eV to 0.172 eV. This indicates greater disorder in the phosphate network with increasing content of CdO. The spectral distribution of the refractive index indicates that the prepared glass acts as a low-dispersion medium in the visible region. Other physical parameters such as the extinction coefficient, optical conductivity, the complex dielectric constant are calculated. The results reveal the role of CdO as a network modifier in the phosphate glass.

ACKNOWLEDGMENT

Deep thanks to Dr. Ahmed El-Basaty, Faculty of Industrial Education, Helwan University; for his help and facilitating the use the equipment for preparing the glass samples.

REFERENCES

1. J. Fuxi Gan, Lei Xu, "Photonic Glasses", World Scientific Publishing Company, 2006.
2. J. Ahmed, M. Lewis, J. Olsen, J.C. Knowles, "Phosphate glasses for tissue engineering: Part 1. Processing and characterisation of a ternary-based $\text{P}_2\text{O}_5\text{-CaO-Na}_2\text{O}$ glass system", *Biomaterials*, vol. 25, pp. 491-499, 2004.
3. Z.M. Da Costa, W.M. Pontuschka, J.M. Giehl, C.R. Da Costa, "ESR dosimeter based on $\text{P}_2\text{O}_5\text{-CaO-Na}_2\text{O}$ glass system", *J. Non-Cryst. Solids*, vol. 352, pp. 3663-3667, 2006.



4. P.K. Jha, O.P. Pandey, K. Singh, "FTIR spectral analysis and mechanical properties of sodium phosphate glass-ceramics", *J. Molec. Struct.*, vol. 1083, pp. 278-285, 2015.
5. I. Soltani, S. Hraiech, K. Horchani-Naifer, H. Elhouichet, B. Gelloz, M. Férid, "Growth of silver nanoparticles stimulate spectroscopic properties of Er³⁺ doped phosphate glasses: Heat treatment effect" *J. Alloy. Comp.*, vol. 686, pp. 556-563, 2016.
6. S. Ibrahim, M.A. Marzouk, G.M. El komy, "Structural Characteristics and Electrical Conductivity of Vanadium-doped lithium Ultraphosphate Glasses" *Silicon*, vol. 9, 403-410, 2017.
7. R.K. Brow, "Review: the structure of simple phosphate glasses", *J. Non-Cryst. Solids*, vol. 263-264, pp. 1-28, 2000.
8. M. Ashraf Chaudhry, Shakeel Bilal, "Concentration-dependent electrical conductivity of phosphate glasses containing zinc oxide", *Mater. Chem. Phys.*, vol. 41, pp. 299-301, 1995.
9. Y. H. Elbashar, Aly Saeed, S. S. Moslem, "Spectroscopic analysis of copper calcium phosphate glasses matrix", *NLOQO*, vol. 48, pp. 41-48, 2016.
10. Y.M. Moustofa, K. El-Egili, "Infrared spectra of sodium phosphate glasses", *J. Non-Cryst. Solids*, vol. 240, pp. 144-153, 1998.
11. M. Altaf, M.A. Chaudhry. "Physical properties of sodium cadmium phosphate glasses." *Inter. J. Modern Phys. B*, vol. 25, pp. 3503-3512, 2011.
12. X. Li, H. Yang, X. Song, Y. Wu, " Glass forming region, structure and properties of zinc iron phosphate glasses" *J. Non-Cryst. Solids*, vol. 379, pp. 208-213, 2013.
13. K.A. Matori, M.H.M. Zaid, H.J. Quah, S.H. Abdul Aziz, Z. Abdul Wahab, M.S.M. Ghazali, "Studying the Effect of ZnO on Physical and Elastic Properties of (ZnO)_x(P₂O₅)_{1-x} Glasses Using Nondestructive Ultrasonic Method", *Adv. Mater. Sci. Eng.*, vol. 2015, Article ID 596361, 6 pages 2015., <http://dx.doi.org/10.1155/2015/596361>.
14. H.M. Mokhtar, S. Saad, A. Abd El-ghany, N.H. Mousa, M. Elokr, "A Study of Electron Paramagnetic Resonance on Copper Ions on Alkali-Alkali Earth Zinc Phosphate Glass", *Amer. J. Phy. App.*, vol. 3, pp. 92-96, 2015.
15. H. Elhaes, M. Attallah, Y. Elbashar, M. El-Okar, M. Ibrahim, "Application of Cu₂O-doped phosphate glasses for bandpass filter" *Physica B: Cond. Matt.*, vol. 449, pp. 251-254, 2014.
16. D.A. Rayan, Y.H. Elbashar, M.M. Rashad, A. El-Korashy, "Optical spectroscopic analysis of cupric oxide doped barium phosphate glass for bandpass absorption filter" *J. Non-Crys. Solids*, vol. 382, pp. 52-56, 2013.
17. Y.H. Elbashar, D.A. Rayan, M.M. Rashad, "Protection glass eyewear against a YAG laser based on a bandpass absorption filter", *Silicon*, vol. 9, pp. 111-116, 2017.
18. Y.H. Elbashar, H.A. Abd El-Ghany, "Optical spectroscopic analysis of Fe₂O₃ doped CuO containing phosphate glass", *Opt. Quant. Electron.*, vol. 49:310, pp. 1-13, 2017. [doi.org/10.1007/s11082-017-1126-0](http://dx.doi.org/10.1007/s11082-017-1126-0).
19. R.E. Pavai, P.S. Dharsini, "Effect of Na₂O on structural and thermal properties of cadmium borate glasses", *IOSR J. App. Phy.*, vol. 9, pp. 67-70, 2017.
20. C.A. Hogarth and M.A. Ghauri, The electrical properties of cadmium phosphate glasses at high electric fields, *J. Mater. Sci.*, vol. 14, pp. 409-414, 1980.



21. I. Pal, A. Agarwal and S. Sanghi, "Spectral analysis and structure of Cu²⁺ doped cadmium bismuth borate glasses", *Ind. J. Pure Appl. Phys.*, vol. 50, pp. 237-244, 2012.
22. J. Chung, J. Kim, S. Choi, H. Park, M. Hwang, Y. Jeong, B. Ryu, "Structural, Optical, and Chemical Properties of Cadmium Phosphate Glasses", *J. Korean Ceramic Soc.*, vol. 52, pp. 128-132, 2015.
23. N. Aboufotouh, Y. Elbashar, M. Ibrahim, M. Elokr, "Characterization of copper doped phosphate glasses for optical applications", *Ceram. Int.*, vol. 40, pp. 10395-10399, 2014.
24. C.R. Osterwald, "Degradation in weathered crystalline-silicon PV modules apparently caused by UV radiation", in *Proceedings of the 3rd World Conference on Photovoltaic Energy Conversion*, Osaka, Japan, 2003, vol. 3, pp. 2911-2915.
25. C.G. Zimmermann, "Time dependent degradation of photovoltaic modules by ultraviolet light" *Appl. Phys. Lett.*, vol. 92, pp. 241110, 2008.
26. M. Tayyib, J.O. Oddenb, T.O. Saetrea, "UV-induced degradation study of multicrystalline silicon" *Energy Procedia*, vol. 38, pp. 626-635, 2013.
27. W.H. Holley, S.C. Agro, J.P. Galica, L.A. Thoma, R.S. Yorgensen, M. Ezrin, P. Klemchuk, G. Lavigne, "Investigation into the causes of browning in EVA encapsulated flat plate PV modules," in *Conference Record of the 24th IEEE Photovoltaic Specialists Conference*, Waikoloa, HI, 1994, vol. 1, pp. 893-896.
28. E. Skoplaki, J.A. Palyvos, "On the temperature dependence of photovoltaic module electrical performance: A review of efficiency/power correlations" *J. Solar Energy*, vol. 83, pp. 614-624, 2009.
29. S. Dubey, J.N. Sarvaiya, B. Seshadri, "Temperature Dependent Photovoltaic (PV) Efficiency and Its Effect on PV Production in the World – A Review" *Energy Procedia*, vol. 33, pp. 311- 321, 2013.
30. Shelby, J.E.: *Introduction to Glass Science and Technology*, 2nd edn. The Royal Society of Chemistry, London, 2005.
31. C. Dayanand, G. Bhikshamaiah, M. Salagram, "IR and optical properties of PbO glass containing a small amount of silica", *Mater. Lett.*, vol. 23, pp. 309-315, 1995.
32. V. Sharma, S. Singh, G. Mudahar, K. Thind, "Synthesis and characterization of cadmium containing sodium borate glasses", *New J. Glass Ceram.*, vol. 2, pp. 128-132, 2012.
33. A.S. Rao, Y.N. Ahammed, R.R. Reddy, T.V.R. Rao, "Spectroscopic studies of Nd³⁺-doped alkali fluoroborophosphate glasses" *Opt. Mater.*, vol. 10, pp. 245-252, 1998.
34. S.A. Siddiqi, M. Masih, A. Mateen, "Optical band gap in Cd-Mn-phosphate glasses Materials", *Mater. Chem. Phys.*, vol. 40, pp. 69-72, 1995.
35. M. Altaf, M.A. Chaudhry, S.A. Siddiqi, "Effect of Li₂O on the Refractive Index and Optical Band Gap of Cadmium Phosphate Glasses", *Glass Phys. Chem.*, vol. 31, pp. 597-601, 2005.
36. K. Subrahmanyam, M. Salagram, "Optical band gap studies on (55 - x)Na₂O - xPbO - 45P₂O₅ (SLP) glass system" *Opt. Mater.*, vol. 15, pp. 181-186, 2000.
37. Y.H. Elbashar, "Structural and spectroscopic analyses of copper doped P₂O₅-ZnO-K₂O-Bi₂O₃ glasses", *Process. App. Ceramics*, vol. 9, pp. 169-173, 2015.
38. S.K.J. Al-Ani, I.H.O. Al-Hassany and Z.T. Al-Dahan, "The optical properties and a.c. conductivity of magnesium phosphate glasses", *J. Mater. Sci.*, vol. 30, pp. 3720-3729, 1995.



39. M. Altaf and M. A. Chaudhry, "Effect of MnO on the Optical Band Gap in MnO-CdO-P₂O₅ Glasses", J. Korean Phys. Soc., vol. 36, pp. 265-268, 2000.
40. M. Nadeem, W. Ahmed, "Optical Properties of ZnS Thin Films", Turk. J. Phys., vol. 24, pp. 651-659, 2000.
41. J. Simmons , K.S. Potter, "Optical Materials", Academic Press; 1 edition, 1999.
42. J.I. Pankove, "Optical Processes in Semiconductors", New York: Dover, 1975.
43. P. Sharma, S.C. Katya, "Determination of optical parameters of a-(As₂Se₃)₉₀Ge₁₀ thin film", J. Phys. D: Appl. Phys., vol. 40, pp. 2115-2120, 2007.